Available online at www.sciencedirect.com
ScienceDirect
Journal of Power Sources 161 (2006) 1056–1061
JOURNAL OF POWER SOURCES
www.elsevier.com/locate/jpowsour

$Ni_{1-x}Cu_x$ alloy-based anodes for low-temperature solid oxide fuel cells with biomass-produced gas as fuel

Zhen Xie [a], Changrong Xia [a,*], Mengying Zhang [a], Wei Zhu [a,b], Huanting Wang [b]

[a] *Laboratory for Biomass Clean Energy, Department of Materials Science and Engineering, University of Science and Technology of China, Hefei, Anhui 230026, China*

[b] *Department of Chemical Engineering, Monash University, Clayton, Vic. 3800, Australia*

Received 12 April 2006; received in revised form 15 May 2006; accepted 16 May 2006
Available online 7 July 2006

Abstract

Ni–Cu alloy-based anodes, $Ni_{1-x}Cu_x$ ($x = 0$, 0.05, 0.2, 0.3)–$Ce_{0.8}Sm_{0.2}O_{1.9}$ (SDC), were developed for direct utilization of biomass-produced gas in low-temperature solid oxide fuel cells (LT-SOFCs) with thin film $Ce_{0.9}Gd_{0.1}O_{1.95}$ electrolytes. The alloys were formed by *in situ* reduction of $Ni_{1-x}Cu_xO_y$ composites synthesized using a glycine-nitrate technique. The electrolyte films were fabricated with a co-pressing and co-firing technique. Electrochemical performance of the $Ni_{1-x}Cu_x$–SDC anode supported cells was investigated at 600 °C when humidified (3% H_2O) biomass-produced gas (BPG) was used as the fuel and stationary air as the oxidant. With Ni–Cu alloys as anodes, carbon deposition was substantially suppressed and electrochemical performance of the cells was sustained for much longer periods of time. For example, the power export of a Ni–SDC supported cell was only 50% of the initial value (200 mW cm^{-2} at 0.5 V) after 20 min, while $Ni_{0.8}Cu_{0.2}$–SDC supported cells could maintain 90% of the initial power density (250 mW cm^{-2} at 0.5 V) over a period of 10 h. The improved performance of the Ni–Cu alloy-based anodes is worth considering in developing SOFCs fueled directly with dilute hydrocarbons such as gases derived from biomass.

Keywords: Solid oxide fuel cells; Low-temperature SOFCs; Biomass-produced gas (BPG); Glycine-nitrate technique; Ni–Cu alloy

1. Introduction

Biomass offers the largest global exploitation potential among different renewable energy sources. Biomass-produced gas (BPG, or gases derived from biomass) comes from gasification, pyrolysis, or anaerobic digestion of biomass. It is a complex mixture composed mainly of hydrogen, methane, carbon monoxide, carbon dioxide and nitrogen [1]. Due to the fact that O^{2-} anions are the species transported through electrolyte membranes, solid oxide fuel cells (SOFCs) could be an appropriately safe, quiet and high efficient conversion technology for BPG. Consequently, operation of SOFCs with BPG as the fuel has been an active research area in recent years. A general problem associated with such fuel cells is the complex fuel composition, depending on both biomass resources and BPG production technologies. Some gases contain a large fraction of CO_2 or a low level of hydrocarbons. These compositions might be in the region where carbon deposition is thermodynamically prohibited. Such BPG can be fed directly to SOFCs with conventional nickel-based anodes in which nickel provides electronic conductivity and catalytic activity [2,3]. For other compositions that have high loading of hydrocarbons (mainly CH_4), carbon deposition can be an important issue when the gases are supplied directly to the nickel-based anodes since nickel is also very active for catalytic dehydrogenation of hydrocarbons. In order to avoid carbon deposition, reforming is proposed for these gases [4,5]. Reforming is critical when coke is formed on the Ni-based anodes using concentrated hydrocarbon fuels such as nature gas or gasoline. However, the concentration of hydrocarbons in BPG is low since they are diluted with CO, CO_2 and N_2. Therefore, it is reasonable to assume that carbon deposition with BPG is moderate, at least not as severe as that with natural gas. If this moderate coke formation can be further catalytically minimized and/or removed, it is possible to feed BPG directly into SOFCs without reforming although the composition is thermodynamically favorable for carbon formation. Here we report our efforts

* Corresponding author. Tel.: +86 551 3607475; fax: +86 551 3606689.
E-mail address: xiacr@ustc.edu.cn (C. Xia).

0378-7753/$ – see front matter © 2006 Elsevier B.V. All rights reserved.
doi:10.1016/j.jpowsour.2006.05.025

to minimize carbon deposition by alloying Ni with Cu since Cu is a poor catalyst for C–C bond formation. While it is possible to minimize carbon deposition by using Ni–Cu alloys as anodes for direct BPG SOFCs, it is also expected that these Ni-rich alloy-based anodes could maintain high catalytic activity comparable to that of conventional Ni-based anodes.

In this work, the alloys were formed by *in situ* reduction of NiO–CuO composites prepared by a glycine nitrate process. The alloy-based anodes were characterized at 600 °C in low-temperature SOFCs fueled with BPG produced by gasification of rice husk [6]. The composition is CO (23.5%), CO_2 (14.3%), H_2 (15.7%), CH_4 (6.2%), and N_2 (40.3%). This composition is in the region where carbon deposition is thermodynamically preferred below 700 °C according to the C–H–O phase diagram reported by Eguchi et al. [7].

2. Experimental

The cells studied in this work consisted of $Ni_{1-x}Cu_x$ ($x = 0$, 0.05, 0.2, 0.3)–$Ce_{0.8}Sm_{0.2}O_{1.9}$ (SDC) anodes, $Ce_{0.9}Gd_{0.1}O_{1.95}$ (GDC) electrolytes and $Sm_{0.5}Sr_{0.5}CoO_3$ (SSC)–SDC cathodes. Oxide powders for fuel cell components including $Ni_{1-x}Cu_xO_y$, SDC, GDC and SSC were prepared using a glycine-nitrate combustion method [8] with nitrate precursors of $Ni(NO_3)_2$, $Cu(NO_3)_2$, $Co(NO_3)_2$, $Sm(NO_3)_3$, $(NH_4)_2Ce(NO_3)_6$, $Gd(NO_3)_3$, and $Sr(NO_3)_2$. Stoichiometric amounts of nitrates were dissolved in distilled water to form a precursor solution. Glycine (NH_2–CH_2–COOH) was then added to the solution. The molar ratio of glycine to nitrate was 1:2. The solution was subsequently heated on a hot plate until it was ignited, producing a metal-oxide 'ash'. The ash was then heated at a temperature above 600 °C to remove possible carbon residues and to form a well-crystalline oxide powder.

Anode supported cells with GDC as electrolytes were prepared using a co-pressing and co-firing technique [9]. Anode powders consisted of $Ni_{1-x}Cu_xO_y$ ($x = 0$, 0.05, 0.2, 0.3) and SDC (the volume ratio of the reduced metal was 50%) were prepared by mixing and grinding the metal oxides and SDC with an agate mortar and pestle. To fabricate a single cell, $Ni_{1-x}Cu_xO_y$–SDC anode powder was first pressed as a substrate. GDC powder was then added onto the substrate and co-pressed again at 280 MPa to form a bilayer. The bilayer was subsequently co-fired at 1000 °C for 2 h. A slurry consisting of SSC–SDC (30 wt.% SDC) and a binder was then screen-printed onto the electrolyte surface and then fired at 950 °C in air for 2 h to form a porous cathode. The cathode fabricating process was kept as consistent as possible so that the cathodic polarization resistance was the same.

In order to estimate the cell performance, single cells were sealed in alumina tubes with silver paste [9]. The paste was sandwiched between the surfaces of the alumina tube and the anode. Care was taken to ensure that no paste was put on the active area of the anode to avoid the possible catalytic contribution of silver. The metal oxides in anode layers were reduced to metal Ni or Cu *in situ* with H_2 at 600 °C before the electrochemical measurements. Electrochemical characterizations were performed at 600 °C. Humidified (3% H_2O) hydrogen or BPG was used as the fuel and stationary air as the oxidant. A Zahner IM6e electrochemical workstation was used to characterize the single cells. The fuel cell performance based on the linear *I–V* curve was measured in the galvanostatic mode. The measurement was conducted after each testing condition (temperature and fuel change) was held for more than 30 min. ac impedance was also measured under open circuit conditions in the frequency range from 0.1 Hz to 1 MHz with 5 mV as the excitation ac amplitude. The stabilities were obtained in the potentiostatic mode at a voltage of 0.5 V.

After reducing the bimetal oxide and NiO powders in H_2 at 600 °C, the alloy and Ni metal phases were determined by powder X-ray diffraction (XRD) with a Philips X'pert PRO S diffractometer. After the cell performance measurements, the microstructures of the anodes were revealed by scanning electron microscope (SEM) using a FEI XL30 Environmental scanning electron microscope.

3. Result and discussion

Shown in Fig. 1a is the XRD pattern with 2θ from 40 to 55° for $Ni_{1-x}Cu_x$ ($x = 0$, 0.05, 0.2, 0.3) metals as obtained by reduc-

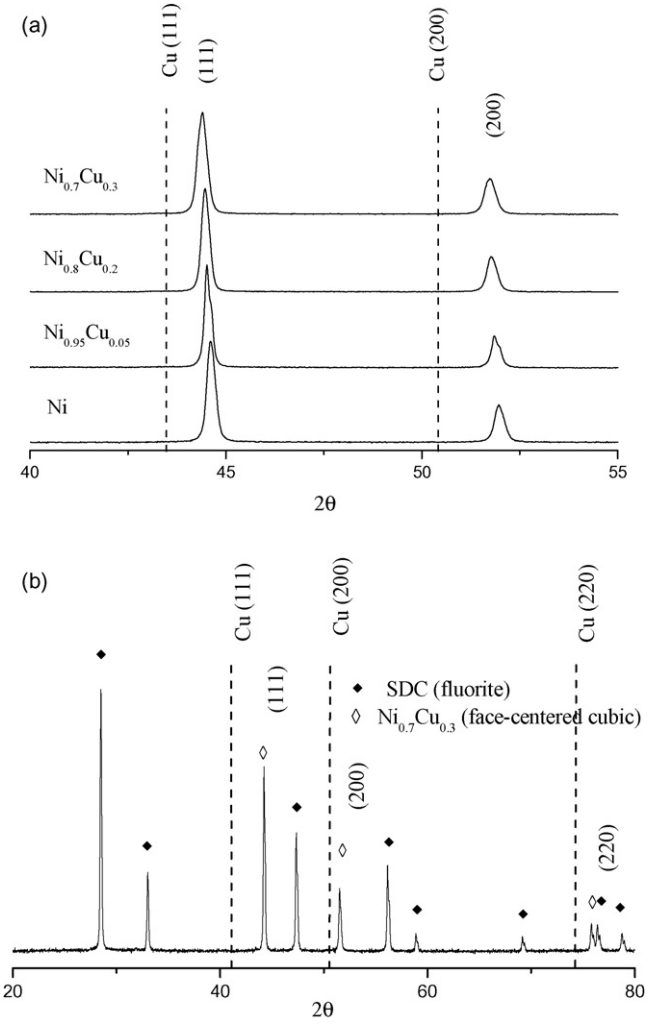

Fig. 1. XRD pattern of Ni–Cu bimetals prepared by reduction of (a) $Ni_{1-x}Cu_xO_y$ composites and (b) $Ni_{0.7}Cu_{0.3}O_y$–SDC.

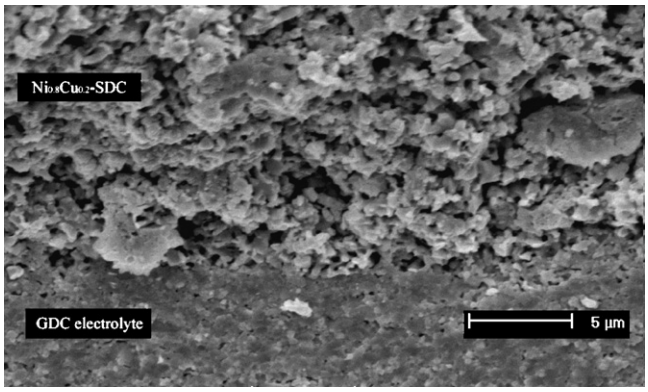

Fig. 2. SEM micrographs for the cross-sectional view of a fresh fuel cell.

ing the $Ni_{1-x}Cu_xO_y$ composites. Diffraction data of pure Cu is also shown in the figure with dotted lines (JCPDS03-1005). It is clear that the diffraction characteristics corresponding to Cu are not observable, implying the formation of only Ni–Cu alloys on reducing the $Ni_{1-x}Cu_xO_y$ composites. The diffraction peaks of these alloys match the (1 1 1) and (2 0 0) characteristics of fcc structure Ni. However, the FCC peaks shifted to low angles with the increase of Cu content. The shifting is expected since the atomic radius of Cu ($r = 128$ pm) is bigger than that of Ni ($r = 124$ pm) [10]. The alloy formation is further shown in Fig. 1b, the XRD pattern of a $Ni_{0.7}Cu_{0.3}$–SDC cermet, which indicates that SDC powder did not separate out CuO and NiO when both $Ni_{1-x}Cu_xO_y$ and SDC were mixed and ground for fuel cell processing. Fig. 2 shows the cross-sectional view of a fresh cell with a $Ni_{0.8}Cu_{0.2}$–SDC anode. The anode is porous, and bonds strongly to the electrolyte. No cross-membrane cracks or open pores were revealed in the electrolyte layer.

Shown in Fig. 3 is the voltage and power density as a function of current density for cells with the $Ni_{1-x}Cu_x$–SDC anodes. The cells were operated at 600 °C with humidified (3% H_2O) hydrogen as the fuel and stationary air as the oxidant. The *I–V* relationships gave straight lines with typical open circuit voltages (OCVs) for cells with doped ceria as electrolytes [9,11–13]. The maximum power densities for Ni–SDC, $Ni_{0.95}Cu_{0.05}$–SDC, $Ni_{0.8}Cu_{0.2}$–SDC and $Ni_{0.7}Cu_{0..3}$–SDC supported cells were 500, 570, 460 and 420 mW cm^{-2}, respectively. It is clear that the $Ni_{0.95}Cu_{0.05}$–SDC supported cell shows the highest power density and yields improved performance compared with the Ni–SDC supported cell. This result is consistent with that reported by Ringuedé et al. [14], who found enhanced performance of Ni-based anodes with small amounts of Cu. This Cu addition might have positive effects on the anodic microstructures and catalytic activity. It can also be seen that the cell performance decreases when the Cu content exceeds 5%. This is possible due to the fact that the catalytic activity of Cu is lower than that of Ni for the electrochemical oxidation of the fuel [15].

Shown in Fig. 4 is the voltage and power density as a function of current density for $Ni_{1-x}Cu_x$–SDC supported cells that operated at 600 °C with humidified (3% H_2O) BPG as the fuel. OCVs for cells with $Ni_{0.95}Cu_{0.05}$–SDC, $Ni_{0.8}Cu_{0.2}$–SDC and $Ni_{0.7}Cu_{0.3}$–SDC anodes are 0.90, 0.89 and 0.86 V, respectively, which are very close to the theoretical values [2]. The maximum power densities for $Ni_{0.95}Cu_{0.05}$–SDC, $Ni_{0.8}Cu_{0.2}$–SDC and $Ni_{0.7}Cu_{0.3}$–SDC supported cells are 350, 250 and 190 mW cm^{-2}, respectively. Comparing Fig. 4 with Fig. 3, it can be seen that the power density of a cell with BPG as the fuel is lower than that of the same cell with H_2 as the fuel. Nevertheless, the cell performance decreases with the increase of Cu content, regardless of the fuel compositions. Shown in Fig. 5 are electrode impedance spectra measured under open circuit conditions for $Ni_{1-x}Cu_x$–SDC supported cells using humidified (3% H_2O) BPG as the fuel. Area specific resistance (ASR), which is the difference between the intercepts on the real axis at high and low frequency, represents the cathode and anode contribution to the interfacial polarization resistance. As shown in Fig. 5, ASRs for $Ni_{0.95}Cu_{0.05}$–SDC, $Ni_{0.8}Cu_{0.2}$–SDC, and $Ni_{0.7}Cu_{0..3}$–SDC supported cells are 0.38, 0.73, and 0.80 Ω cm^2,

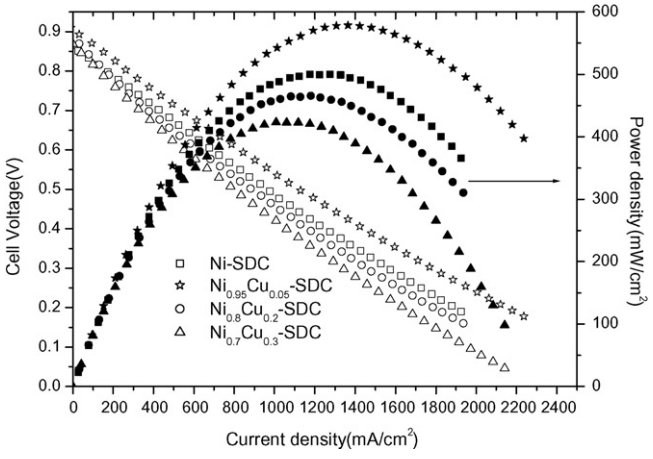

Fig. 3. Cell voltage (open symbols) and power density (solid symbols) vs. current density for cells with $Ni_{1-x}Cu_x$–SDC anodes. Measurements were conducted at 600 °C with humidified (3% H_2O) hydrogen as the fuel and stationary air as the oxidant.

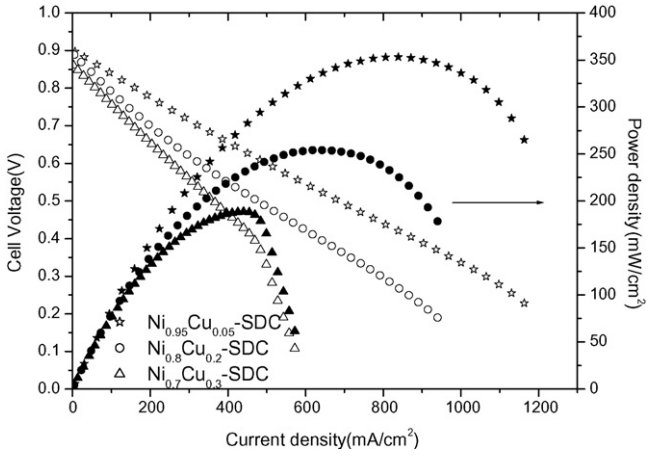

Fig. 4. Cell voltage (open symbols) and power density (solid symbols) vs. current density for cells with $Ni_{1-x}Cu_x$–SDC anodes. Measurements were conducted at 600 °C with humidified (3% H_2O) BPG as the fuel and stationary air as the oxidant.

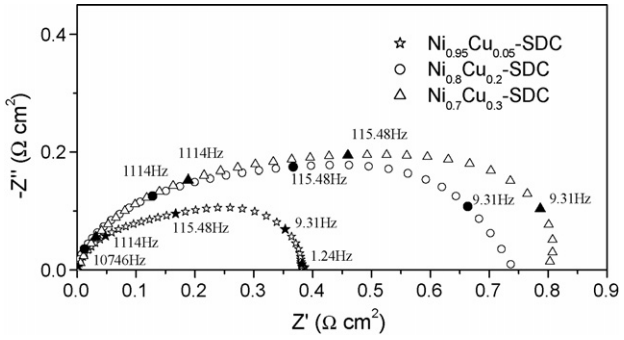

Fig. 5. Electrode impedance spectra measured at 600 °C in open circuit conditions for $Ni_{1-x}Cu_x$–SDC ($x = 0.05$, 0.2, 0.3) supported cells with humidified (3% H_2O) BPG as the fuel.

respectively. Since the cathodes are identical, the differences in ASR can be essentially attributed to the anode. Therefore, it is clear that the interfacial polarization resistance of $Ni_{0.95}Cu_{0.05}$–SDC anode is the lowest; 0.35 and 0.42 Ω cm^2 lower than that of $Ni_{0.8}Cu_{0.2}$–SDC and $Ni_{0.7}Cu_{0.3}$–SDC, respectively. So both the *I–V* and impedance measurements show that the cell performance decreases when more Cu is added to the Ni-based anodes for direct utilization of BPG. It could also be attributed to the relatively lower catalytic activity of Cu than that of Ni. In addition, replacing nickel with copper might change the microstructure of the Ni-based anode when the cell is fabricated with a co-firing process. As shown in Fig. 4, a diffusion limitation is obvious for the $Ni_{0.7}Cu_{0.3}$–SDC supported cell while it does not exist for $Ni_{0.95}Cu_{0.05}$–SDC and $Ni_{0.8}Cu_{0.2}$–SDC supported cells, implying that the anode porosity decreases with the increase in Cu content. However, when H_2 is used as the fuel, this limitation is not observed, possibly due to the high fuel loading.

Shown in Fig. 6 are the power densities of $Ni_{1-x}Cu_x$–SDC ($x = 0$, 0.05, 0.2, and 0.3) supported cells with a constant cell voltage of 0.5 V. The cells were operated at 600 °C with humidified BPG as the fuel. The performance of the Ni–SDC supported cell decreased rapidly with time and the power density was only 50% of the initial value after 20 min. It should be noted that the initial power density of the Ni–SDC supported cell (200 mW cm^{-2} at 0.5 V) was lower than that of the $Ni_{0.8}Cu_{0.2}$–SDC supported cell (250 mW cm^{-2} at 0.5 V) when using BPG as the fuel, while the power export of the former cell was higher than that of the $Ni_{0.8}Cu_{0.2}$–SDC supported cell when using H_2 as the fuel. This was possibly caused by rapid deterioration in catalytic activity of the Ni–SDC anode in the presence of BPG considering that the data was recorded 30 min after the fuel was switched from H_2 to BPG. Improvement in stability was achieved by partial replacing Ni with Cu. When 5% Ni is replaced, the exported power decreased only 3% after 60 min, and 20% after 10 h. Further, the cell could maintain 90% of the initial power density over a period of 10 h when 20% and 30% Ni was replaced, respectively. The results show that it is very effective to increase the stability of a fuel cell with direct utilization of BPG by adding copper to the conventional Ni-based cermet anode. However, further improvement in stability is required for commercial usage of SOFCs.

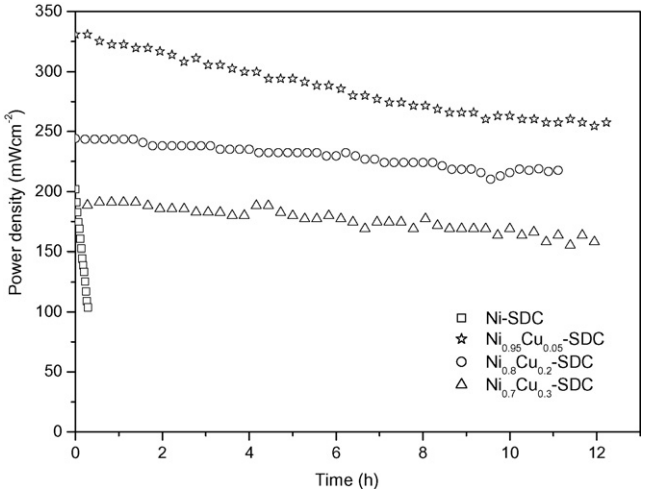

Fig. 6. Power densities of $Ni_{1-x}Cu_x$–SDC ($x = 0$, 0.05, 0.2, 0.3) supported cells that operated at 600 °C with a fixed cell voltage when humidified (3% H_2O) BPG was used as the fuel.

Shown in Fig. 7 are the impedance spectra measured at 600 °C under open circuit conditions for the $Ni_{0.8}Cu_{0.2}$–SDC supported cell before and after 11 h operating directly with humidified BPG as the fuel. The electrolyte resistance, the high frequency intercept at the real axis, did not change with time. Meanwhile, the electrode polarization resistance decreased 0.08 Ω cm^2 after 11 h testing with BPG. Comparing the two impedance spectra for the polarization resistance it could be found that the low frequency part shrunk after the test whereas the high frequency part was unchanged. It has been reported that the anode polarization resistance contributes to the low frequency part of the impedance measured with a two-wire configuration [16]. Consequently, the anode polarization resistance decreased after the test. This is possibly caused by the formation of carbon deposits, which enhance the electronic conductivity of the anode. The decrease of the anode polarization resistance as an effect of the carbon deposition has been well described by Gorte and coworkers [17], who have reported work on direct utilization of hydrocarbons in SOFCs. Shown in Fig. 8 is the performance

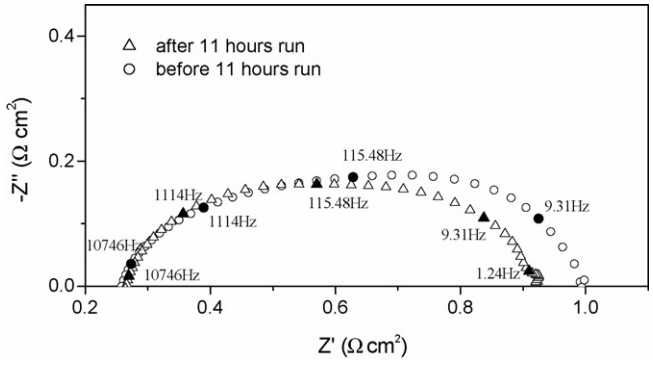

Fig. 7. Impedance spectra measured at 600 °C under open circuit conditions for $Ni_{0.8}Cu_{0.2}$–SDC supported cell after and before 11 h run with humidified (3% H_2O) BPG as the fuel.

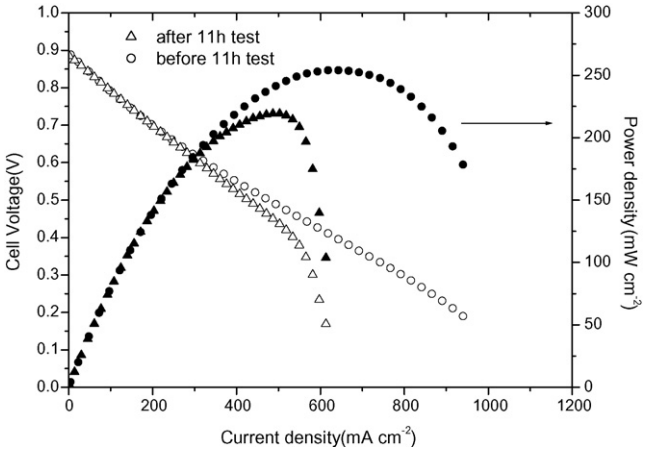

Fig. 8. Cell voltage and power density as a function of current density for $Ni_{0.8}Cu_{0.2}$–SDC supported cell with humidified (3% H_2O) BPG as the fuel. The measurement was conducted at 600 °C before and after the cell was tested with humidified (3% H_2O) BPG as the fuel for 11 h.

of the $Ni_{0.8}Cu_{0.2}$–SDC supported cell with BPG as the fuel. The data was obtained before and after 11 h test with BPG. It is obvious that diffusional limitations began to affect the cell performance even though a decrease in anode polarization resistance was observed in the open circuit condition. The limitation must have been caused by carbon deposits, which subsequently blocked the anode pores.

Carbon formation on the $Ni_{0.8}Cu_{0.2}$–SDC anode is further shown in Fig. 9a and b. Fig. 9a displays the surface microstructure of a fresh $Ni_{0.8}Cu_{0.2}$–SDC anode and Fig. 9b the $Ni_{0.8}Cu_{0.2}$–SDC anode that has been tested with BPG for 11 h. Isolated deposits could be found on the surface of the used anode by comparing the two SEM photos. The deposits proved to be carbon as analyzed with elemental dot mapping. Although carbon deposits were still found on the $Ni_{0.8}Cu_{0.2}$–SDC anode, the deposition rate was significantly reduced compared with that on a Ni–SDC anode. Shown in Fig. 9c and d are the SEM graphs for the surface microstructure of a fresh Ni–SDC cermet and a Ni–SDC anode that has been tested with BPG for 20 min. The particle size of a fresh Ni–SDC cermet was much smaller than that of a fresh $Ni_{0.8}Cu_{0.2}$–SDC though they were fabricated with an identical process. Further particle growth of the $Ni_{0.8}Cu_{0.2}$–SDC cermet is possibly due to the low melting point of copper oxides. As shown in Fig. 9d, large amounts of carbon deposits were formed on the surface of Ni–SDC anode, which had been used for only 20 min with BGP as the fuel. The carbon deposits covered almost all the particles of the anode and formed a continuous layer, which obstructed gas transportation and thus caused a diffusional overpotential for the anode. This eventually resulted in the bad performance as shown in Fig. 6. Comparing Fig. 9b with Fig. 9d, it is clear that carbon deposition has been substantially suppressed by replacing Ni with a Ni–Cu alloy containing 20% Cu. This indicates that carbon deposition is more likely formed as an effect of kinetics than thermodynamics. However, when biomass-produced gases and hydrocarbon are fed directly to low-temperature SOFCs without pretreatment, the Cu–Ni bimetal anode has to be modified

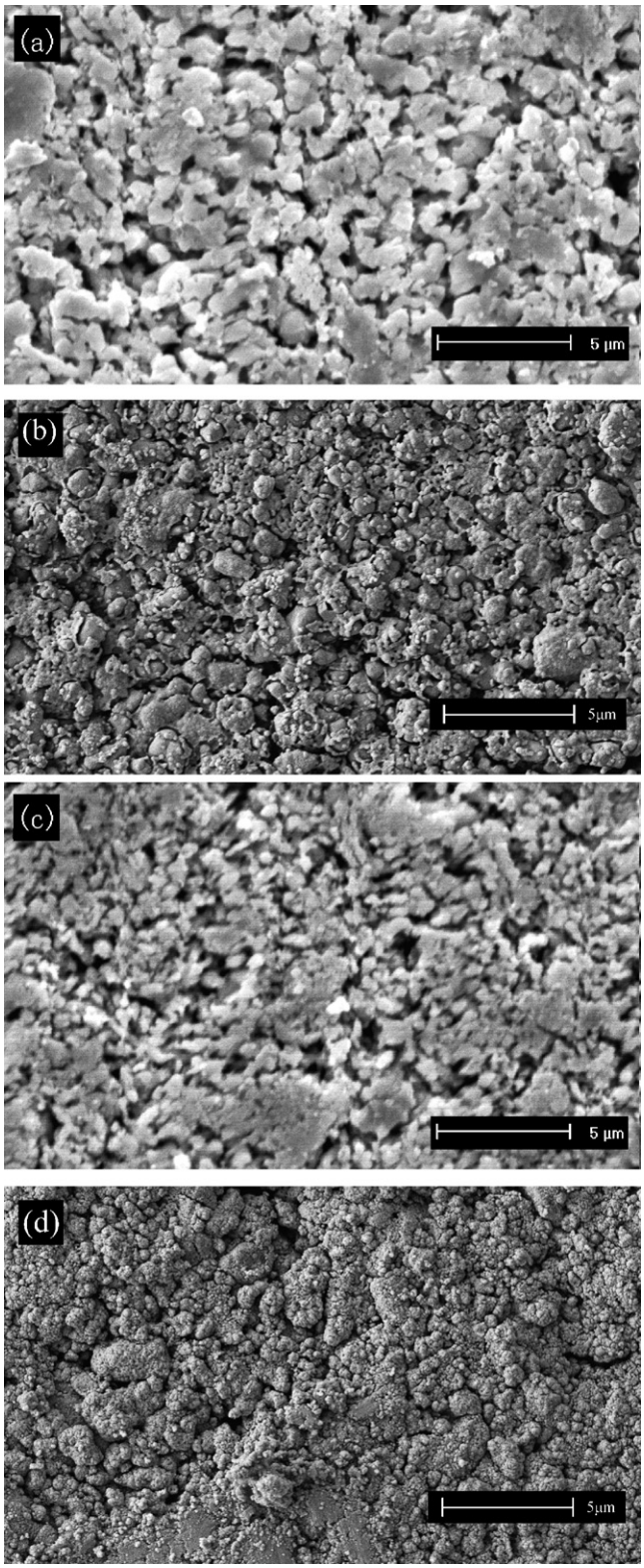

Fig. 9. SEM micrographs for the surface microstructure of (a) a fresh $Ni_{0.8}Cu_{0.2}$–SDC cermet, (b) a $Ni_{0.8}Cu_{0.2}$–SDC cermet after 11 h test with BPG as the fuel, (c) a fresh Ni–SDC cermet and (d) a Ni–SDC cermet after 20 min test with BPG as the fuel.

to further improve its activity to suppress and/or remove carbon deposition.

4. Conclusion

We have demonstrated that it is very effective to increase the stability of a fuel cell with direct utilization of BPG by using Ni–Cu alloy-based anodes. With humidified (3% H_2O) BPG as the fuel, the power density of a Ni–SDC supported cell was only 50% of the initial value after 20 min, while $Ni_{0.8}Cu_{0.2}$–SDC and $Ni_{0.7}Cu_{0.3}$–SDC supported cells could maintain 90% of initial power density over a period of 10 h. The SEM investigation indicates that carbon deposition has been substantially suppressed by replacing Ni with a Ni–Cu alloy. In addition, the *I–V* and impedance measurements show that the cell performance decreased with the increase of Cu content when humidified (3% H_2O) BPG and H_2 were used as the fuel. This can be attributed to the relatively lower catalytic activity of Cu than Ni. Further work will focus on optimizing the performance of these anodes.

Acknowledgements

This work was supported by the Natural Science Foundation of China (50332040 and 50372066) and also by the China Ministry of Education (SRFDP20050358023). HW thanks the Australian Research Council for the QEII Fellowship.

References

[1] A. Demirbas, Energy Convers. Manage. 42 (2001) 1357–1378.
[2] Y.H. Yin, W. Zhu, C.R. Xia, C. Gao, G.Y. Meng, J. Appl. Electrochem. 34 (2004) 1287–1291.
[3] K. Kendall, C.M. Finnerty, G. Saunders, J.T. Chung, J. Power Sources 106 (2002) 323–327.
[4] J. Staniforth, R.M. Ormerod, Catal. Lett. 81 (1/2) (2002) 19–23.
[5] J.V. herle, Y. Membrez, O. Bucheli, J. Power Sources 127 (2004) 300–312.
[6] H. Jiang, X.F. Zhu, Q.X. Guo, Q.S. Zhu, Ind. Eng. Chem. Res. 42 (2003) 5745–5750.
[7] K. Eguchi, H. Kojo, T. Takeguchi, R. Kikuchi, K. Sasaki, Solid State Ionics 152/153 (2002) 411–416.
[8] R.R. Peng, C.R. Xia, Q.X. Fu, G.Y. Meng, D.K. Peng, Mater. Lett. 56 (2002) 1043–1047.
[9] C.R. Xia, M.L. Liu, Solid State Ionics 144 (2001) 249–255.
[10] J.A. Dean, Lange's Handbook of Chemistry, 15th ed., McGraw-Hill, Inc., New York, 1999, pp. 4.31–4.32.
[11] S.W. Zha, W. Rauch, M.L. Liu, Solid State Ionics 166 (2004) 241–250.
[12] S.W. Zha, A. Moore, H. Abernathy, M.L. Liu, J. Electrochem. Soc. 151 (8) (2004) A1128–A1133.
[13] Y.J. Leng, S.H. Chan, S.P. Jiang, K.A. Khor, Solid State Ionics 170 (2004) 9–15.
[14] A. Ringuedé, D.P. Fagg, J.R. Frade, J. Eur. Ceram. Soc. 24 (2004) 1355–1358.
[15] A. Atkinson, S. Barnett, R.J. Gorte, J.T.S. Irivne, A.J. Mcevoy, M. Mogensen, S.C. Singhal, J. Vohs, Nat. Mater. 3 (2004) 17–27.
[16] S. Mclntosh, R.J. Gorte, Chem. Rev. 104 (2004) 4845–4865.
[17] H. Kim, C. Lu, W.L. Worrell, J.M. Vohs, R.J. Gorte, J. Electrochem. Soc. 149 (3) (2002) A247–A250.